JOURNAL OF AGRICULTURAL AND FOOD CHEMISTRY

Synthesis, Herbicidal Activities, and 3D-QSAR of 2-Cyanoacrylates Containing Aromatic Methylamine Moieties

YU-XIU LIU,[†,§,△] DENG-GUO WEI,[§,△] YE-RONG ZHU,[#,△] SHAO-HUA LIU,[†] YONG-LIN ZHANG,[†] QI-QI ZHAO,[†] BAO-LI CAI,[†] YONG-HONG LI,[†] HAI-BIN SONG,[†] YING LIU,*[,§] YONG WANG,*[,#] RUN-QIU HUANG,[†] AND QING-MIN WANG*[,†]

State Key Laboratory of Elemento-Organic Chemistry, Tianjin Key Laboratory of Pesticide Science, Institute of Elemento-Organic Chemistry, Nankai University, Tianjin 300071, China; State Key Laboratory for Structural Chemistry of Unstable and Stable Species, College of Chemistry and Molecular Engineering, Peking University, Beijing 100871, China; and College of Life Sciences, Nankai University, Tianjin 300071, China

A series of novel 2-cyanoacrylates containing different aromatic rings were synthesized, and their structures were characterized by ^{1}H NMR, elemental analysis, and single-crystal X-ray diffraction analysis. Their herbicidal activities against four weeds and inhibition of photosynthetic electron transport against isolated chloroplasts (the Hill reaction) were evaluated. Both in vivo and in vitro data showed that the compounds containing benzene, pyridine, and thiazole moieties gave higher activities than those containing pyrimidine, pyridazine, furan, and tetrahedronfuran moieties. To further explore the comprehensive structure–activity relationship on the basis of in vitro data, comparative molecular field analysis (CoMFA) was performed, and the results showed that a bulky and electronegative group around the para-position of the aromatic rings would have the potential for higher activity, which offered important structural insights into designing highly active compounds prior to the next synthesis.

KEYWORDS: Herbicides; photosynthetic electron transport inhibitors; 2-cyanoacrylates; aromatic rings; CoMFA

INTRODUCTION

2-Cyanoacrylates are inhibitors of photosystem II (PSII) electron transport, which inhibits the growth of weeds by disrupting photosynthetic electron transport at the PSII reaction center. Among these cyanoacrylates, the compound **I-1** (**Table 1**) has been reported to exhibit high inhibitory activity of the Hill reaction (*1–3*). The reported QSAR analysis has focused on 2-cyanoacrylates containing phenyl or benzyl (*4*). In our previous paper (*5*), compound **I-2** (**Table 1**) showed good herbicidal activity, and pyridyl compound **I-3** showed better herbicidal activity. Furthermore, it has been validated that 2-cyanoacrylates with an ethoxyethyl group at the ester moiety have much higher activity than those with any other alkyl group. Thus, some studies on ethoxyethyl cyanoacrylates containing herterocycles were carried out by us to develop better potential herbicides (*6–10*). To study the structure–activity relationship, a series of cyanoacrylates containing phenyl, pyridyl, thiazole, pyridazine, and pyrimidine groups were synthesized and tested for their herbicidal activity. The Hill reaction was conducted to test their electron transport inhibitory ability, and the analysis of the relationships between the structure and the in vitro activity was performed by comparative molecular field analysis (CoMFA) (*11*). Herein we report the new developments.

MATERIALS AND METHODS

Instruments. The melting points of the products were determined on an X-4 binocular microscope (Beijing Tech Instrument Co., Beijing, China) and were not corrected. ^{1}H NMR spectra were obtained at 300 MHz using a Bruker AC-P 300 spectrometer. Chemical shift values (δ) are given in parts per million downfield from the internal standard tetramethylsilane. Elemental analyses were determined on a Yanaca CHN Corder MT-3 elemental analyzer. MS was obtained at high resolution, ESI-FTICR-MS (Ionspec 7.0T).

Synthetic Procedures. 4-Chloro-5-methylbenzene (**IVa**) and 2-chloro-5-chloromethylpyridine (**Vb**) were commercial reagents. Compounds **IIIa**, **IIIb** and **IIIc** (*5*), 2-bromo-5-methylpyridine (**IVc**) (*12*) and 2-bromo-5-methylthiozole (**IVf**) (*13*), 3-chloro-6-methylpyridazine

* Authors to whom correspondence should be addressed [(Wang) telehone +86-(0)22-23499842, fax +86-(0)22-23499842, e-mail wang98h@263.net; (Liu) telephone 86-10-62767284, fax 86-10-62751725, e-mail liuying@pku.edu.cn].

† State Key Laboratory of Elemento-Organic Chemistry.

§ State Key Laboratory for Structural Chemistry of Unstable and Stable Species.

Nankai University.

△ Three authors contributed equally to this work.

10.1021/jf072851x CCC: $40.75
Published on Web 12/04/2007

Table 1. Title Compounds I[a]

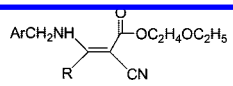

I

No.	Ar	R	No.	Ar	R
I-1*	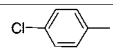	i-Pr	I-18	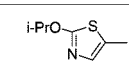	i-Pr
I-2*	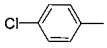	MeS	I-19	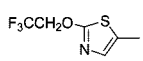	MeS
I-3*	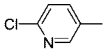	MeS	I-20	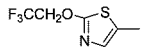	i-Pr
I-4	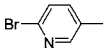	MeS	I-21	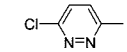	MeS
I-5	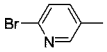	Et	I-22	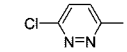	i-Pr
I-6	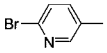	i-Pr	I-23	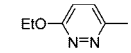	MeS
I-7	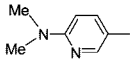	MeS	I-24	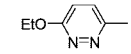	i-Pr
I-8	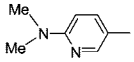	i-Pr	I-25	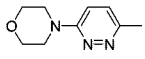	MeS
I-9	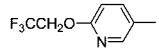	MeS	I-26	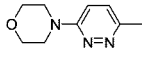	i-Pr
I-10**	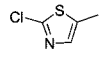	i-Pr	I-27	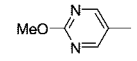	MeS
I-11	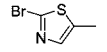	MeS	I-28	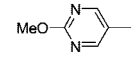	Et
I-12	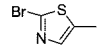	i-Pr	I-29	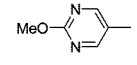	i-Pr
I-13	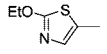	MeS	I-30	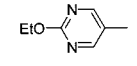	MeS
I-14	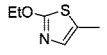	i-Pr	I-31**		MeS
I-15	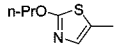	MeS	I-32**		i-Pr
I-16	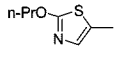	i-Pr	I-33**		i-Pr
I-17	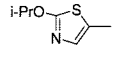	MeS	I-34**		i-Pr

[a] * Compounds **I-1** to **I-3** were not first synthesized, but a different procedure was used in this paper. ** The synthetic procedures of compounds **I-10** (*7*) and **I-31** to **I-34** (*10*) were reported in the cited references.

(**IVk**) (*14*) and 2-chloro-5-methylpyrimidine (**IVn**) (*15*), and 6-chloropyridine-3-carboxamide (**VII**) (*9*) were prepared according to published procedures. Bromomethyl or chloromethyl compounds **V** were synthesized from corresponding **IV** and NBS or NCS (*16*).

General Synthetic Procedures for VIa, VIb, VIc, VIf, VIk, and VIn. To a solution of **V** (0.05 mol) in *N*,*N*-dimethylformamide (20 mL) was added potassium phthalimide (0.05 mol) in a small portion. After the mixture had been stirred at room temperature for 5 h, water (50 mL) was added, and lots of precipitate appeared. The crude product was collected by filtration and washed with water. After recrystallization from ethanol, a white crystal was obtained.

Data for **VIa**: yield, 91.0%; mp, 124–125 °C; ^{1}H NMR ($CDCl_3$), δ 4.85 (s, 2H), 7.29 (d, $^3J_{HH}$ = 8.7 Hz, 2H), 7.38 (d, $^3J_{HH}$ = 8.7 Hz, 2H), 7.70–7.73 (m, 2H), 7.83–7.86 (m, 2H).

Data for **VIb**: yield, 93.3%; mp, 137–139 °C; ^{1}H NMR ($CDCl_3$), δ 4.83 (s, 2H), 7.28 (d, $^3J_{HH}$ = 8.4 Hz, 1H), 7.72–7.77 (m, 3H), 7.84–7.88 (m, 2H), 8.49 (d, $^4J_{HH}$ = 2.4 Hz, 1H).

Data for **VIc**: yield, 90.5%; mp, 139–141 °C; ^{1}H NMR ($CDCl_3$), δ 4.81 (s, 2H), 7.44 (d, $^3J_{HH}$ = 7.6 Hz, 1H), 7.63–7.66 (m, 1H), 7.72–7.75 (m, 2H), 7.85–7.87 (m, 2H), 8.48 (s, 1H). Anal. Calcd for $C_{14}H_9BrN_2O_2$ (%): C, 53.02; H, 2.86; N, 8.83. Found: C, 52.95; H, 2.70; N, 8.60.

Data for **VIf**: yield, 78.0%; mp, 93–95 °C; ^{1}H NMR ($CDCl_3$), δ 4.98 (s, 2H), 7.61 (s, 1H), 7.61–7.76 (m, 2H), 7.85–7.88 (m, 2H).

Data for **VIk**: yield, 79.0%; mp, 202–203 °C; ^{1}H NMR ($CDCl_3$), δ 5.20 (s, 2H), 7.48 (s, 2H), 7.73–7.81 (m, 2H), 7.86–7.95 (m, 2H).

Data for **VIn**: yield, 27.9% (from **IVn**); mp, 182–183 °C; ^{1}H NMR ($CDCl_3$), δ 4.84 (s, 2H), 7.79–7.73 (m, 2H), 7.91–7.85 (m, 2H), 8.75 (s, 2H).

Synthetic Procedure for VIo. To a solution of sodium methoxide (9 mmol) in methanol (20 mL) phthalimide (**VIn**) (3 mmol) was added *N*-(2-chloro-5-pyrimidylmethyl), and the resulting mixture was refluxed for 50 min. After the most of the solvent had been removed in vacuo, the residue was neutralized to pH 7–8 with 1 mol/L hydrochloride acid. The resulting pastelike mixture was filtered and successively washed with water (3 mL) and ethanol (3 mL) to give *N*-(2-methoxy-5-pyrimidylmethyl)phthalimide (**VIo**) as a white solid: yield, 77.5%; mp, 202–203 °C; ^{1}H NMR ($CDCl_3$), δ 3.99 (s, 3H), 4.78 (s, 2H), 7.76–7.70 (m, 2H), 7.89–7.83 (m, 2H), 8.64 (s, 2H). Anal. Calcd for $C_{14}H_{11}N_3O_3$: C, 62.45; H, 4.12; N, 15.61. Found: C, 62.44; H, 3.89; N, 15.41.

Synthetic Procedure for VIp. Compound **VIp** was prepared from **VIn** according to the same method as for **VIo**, which underwent the next reaction without further purification.

General Synthetic Procedures for IIa, IIb, IIc, IIf, IIk, IIo, and IIp. To a suspension of N-substituted phthalimide **VI** (0.04 mol) in ethanol (40 mL) was added hydrazine hydrate (0.5 mL). The reaction mixture was refluxed for 5 h and then cooled. The precipitated phthalyl hydrazide was filtered and washed with ethanol, and then the combined filtrate was condensed under reduced pressure to give crude **II**, which underwent the next reaction without further purification.

Data for **IIa**: crude yield, 91.2%; ^{1}H NMR ($CDCl_3$), δ 1.45 (br s, 2H), 3.83 (s, 2H), 7.22–7.30 (m, 4H).

Data for **IIb**: crude yield, 91.2%; ^{1}H NMR ($CDCl_3$), δ 1.51 (br s, 2H), 4.57 (s, 2H), 7.35 (d, $^3J_{HH}$ = 8.4 Hz, 1H), 7.71 (dd, $^3J_{HH}$ = 8.4 Hz, $^4J_{HH}$ = 2.4 Hz, 1H), 8.40 (d, $^4J_{HH}$ = 2.4 Hz, 1H).

Data for **IIc**: crude yield, 87.4%; ^{1}H NMR ($CDCl_3$), δ 1.44 (br s, 2H), 3.86 (s, 2H), 7.46 (d, $^3J_{HH}$ = 8.1 Hz, 1H), 7.55–7.59 (m, 1H), 8.33 (d, $^4J_{HH}$ = 2.1 Hz, 1H).

Data for **IIf**: crude yield, 98.0%; ^{1}H NMR ($CDCl_3$), δ 1.63 (br s, 2H), 4.05 (s, 2H), 7.39 (s, 1H).

Data for **IIk**: crude yield, 93.0%; mp, 97–98 °C; ^{1}H NMR ($CDCl_3$), δ 1.60 (br s, 2H), 4.13 (s, 2H), 7.42 (d, $^3J_{HH}$ = 9.0 Hz, 1H), 7.49 (d, $^3J_{HH}$ = 9.0 Hz, 1H).

Data for **IIo**: crude yield, 100%; ^{1}H NMR ($CDCl_3$), δ 1.77 (br s, 2H), 3.87 (s, 2H), 4.00 (s, 3H), 8.51 (s, 2H).

Data for **IIp**: crude yield, 100%; ^{1}H NMR ($CDCl_3$), δ 1.89 (br s, 2H), 1.43 (t, $^3J_{HH}$ = 7.2 Hz, 3H), 3.84 (s, 2H), 4.41 (q, $^3J_{HH}$ = 7.2 Hz, 2H), 8.47 (s, 2H).

General Synthetic Procedures for IIe, IIg, IIh, IIi, IIj, and IIl. To corresponding alcohol (10 mL) was added metal sodium (5 mmol). After the sodium disappeared, compound **IIc**, **IIf**, or **IIk** was added, and the mixture was refluxed for 6−24 h monitored by TLC. Then the solvent was evaporated, and the residue was dissolved in methylene dichloride (10 mL) and washed with water. The organic layer was dried and condensed to give corresponding **II**.

Data for **IIe**: crude yield, 78.8%; ^{1}H NMR ($CDCl_3$), δ 1.48 (br s, 2H), 3.84 (s, 2H), 4.75 (q, $^3J_{HF}$ = 8.1 Hz, 2H), 6.83–6.87 (m, 1H), 7.64 (d, $^3J_{HH}$ = 8.4 Hz, 1H), 8.07 (d, $^4J_{HH}$ = 2.4 Hz, 1H).

Data for **IIg**: crude yield, 58.9%; ^{1}H NMR ($CDCl_3$), δ 1.42 (t, $^3J_{HH}$ = 7.2 Hz, 3H), 1.60 (br s, 2H), 3.91 (s, 2H), 4.42 (q, $^3J_{HH}$ = 7.2 Hz, 2H), 6.90 (s, 1H).

Data for **IIh**: crude yield, 70.0%; ^{1}H NMR ($CDCl_3$), δ 1.02 (t, $^3J_{HH}$ = 7.2 Hz, 3H), 1.64 (br s, 2H), 1.76–1.88 (m, 2H), 3.91 (s, 2H), 4.31 (t, $^3J_{HH}$ = 6.6 Hz, 2H), 6.90 (s, 1H).

Data for **IIi**: crude yield, 98.0%; ^{1}H NMR ($CDCl_3$), δ 1.21 (d, $^3J_{HH}$ = 6.3 Hz, 6H), 1.65 (br s, 2H), 3.90 (s, 2H), 5.06–5.18 (m, 1H), 6.90 (s, 1H).

Data for **IIj**: crude yield, 90.0%; ^{1}H NMR ($CDCl_3$), δ 1.69 (br s, 2H), 3.93 (s, 2H), 4.78 (q, $^3J_{HF}$ = 8.1 Hz, 2H), 6.92 (s, 1H).

Data for **IIl**: crude yield, 60.0%; ^{1}H NMR ($CDCl_3$), δ 1.45 (t, $^3J_{HH}$ = 6.9 Hz, 3H), 1.72 (br s, 2H), 4.07 (s, 2H), 4.56 (q, $^3J_{HH}$ = 7.0 Hz, 2H), 6.92 (d, $^3J_{HH}$ = 9.0 Hz, 1H), 7.37 (d, $^3J_{HH}$ = 9.0 Hz, 1H).

Synthetic Procedure for IIm. A mixture of (6-chloropyridazin-3-yl)methylamine (**IIk**) (0.45 g, 3.1 mmol) and morpholine (10 mL) was refluxed for 1 h. Then the excessive morpholine was evaporated, and the residue was dissolved in methylene dichloride (10 mL) and washed with water. The organic layer was dried and condensed to give crude **IIm** as brown oil.

Data for **IIm**: crude yield, 72.0%; ^{1}H NMR ($CDCl_3$), δ 1.70 (br s, 2H), 3.71–3.84 (m, 4H), 3.97 (s, 2H), 4.48–4.58 (m, 4H), 6.84 (d, $^3J_{HH}$ = 9.3 Hz, 1H), 7.20 (d, $^3J_{HH}$ = 9.3 Hz, 1H).

Synthetic Procedure for VIII. A mixture of 6-chloropyrimidine-3-carboxamide (**VII**) (1.74 g, 11.1 mmol), diethylamine (2.67 mL), and DMF (7 mL) was heated to 130 °C for 6 h. Then the mixture was cooled and poured into water. 6-(Dimethylamino)pyrimidine-3-carboxamide (**VIII**) was filtered as a white solid: yield, 34.2%; mp, 231–232 °C; ^{1}H NMR (DMSO-d_6), δ 3.18 (s, 6H), 6.63 (d, $^3J_{HH}$ = 9.0 Hz, 1H), 7.07 (br s, 1H), 7.71 (br s, 1H), 7.91–7.95 (m, 1H), 8.60 (d, $^4J_{HH}$ = 1.8 Hz, 1H). Anal. Calcd for $C_8H_{11}N_3O$ (%): C, 58.17; H, 6.71; N, 25.44. Found: C, 58.29; H, 6.59; N, 25.24.

Synthetic Procedure for IId. To a suspension of $LiAlH_4$ (1.5 g, 40 mmol) in anhydrous tetrahydrofuran (50 mL) was added 6-(dimethylamino)pyrimidine-3-carboxamide (**VIII**) (1.36 g, 8.2 mmol) at 0 °C. The reaction mixture was then stirred at room temperature for 4 h. To the mixture was carefully added aqueous sodium hydroxide to decompose excessive $LiAlH_4$, and the inorganic salt was filtered. The filtrate was diluted with water and extracted with chloroform. The organic layer was dried and concentrated in vacuo to give crude **IId** (1.02 g) as oil: crude yield, 89.0%; ^{1}H NMR ($CDCl_3$), δ 1.60 (br s, 2H), 3.08 (s, 6H), 3.73 (s, 2H), 6.51 (d, $^3J_{HH}$ = 8.7 Hz, 1H), 7.44 (dd, $^3J_{HH}$ = 8.7 Hz, $^4J_{HH}$ = 2.4 Hz, 1H), 8.02 (d, $^4J_{HH}$ = 2.4 Hz, 1H).

General Synthetic Procedures for the Title Compounds I. A mixture of **IIIa** (or **IIIb** or **IIIc**) (5 mmol) and crude **II** (6 mmol) and ethanol (20 mL) was refluxed for 1–3 h (monitored by TLC) and then evaporated under reduced pressure to give crude product. The product was purified by vacuum column chromatography on a silica gel.

Data for **I-1**: yield, 91.1%; mp, 118–120 °C; ^{1}H NMR ($CDCl_3$), δ 1.21 (t, $^3J_{HH}$ = 6.8 Hz, 3H, CH_3), 1.36 (d, $^3J_{HH}$ = 6.8 Hz, 6H, $C(CH_3)_2$), 3.02–3.20 (m, 1H, CH), 3.57 (q, $^3J_{HH}$ = 7.2 Hz, 2H, OCH_2), 3.69 (t, $^3J_{HH}$ = 5.2 Hz, 2H, OCH_2), 4.28 (t, $^3J_{HH}$ = 5.2 Hz, 2H, CO_2CH_2), 4.57 (d, $^3J_{HH}$ = 5.6 Hz, 2H, NCH_2), 7.18 (d, $^3J_{HH}$ = 8.4 Hz, 2H, Ph), 7.35 (d, $^3J_{HH}$ = 8.4 Hz, 2H, Ph), 10.56 (s, 1H, NH).

Data for **I-2**: yield, 95.0%; mp, 72–73 °C; ^{1}H NMR ($CDCl_3$), δ 1.20 (t, $^3J_{HH}$ = 6.8 Hz, 3H, CH_3), 2.66 (s, 3H, SCH_3), 3.56 (q, $^3J_{HH}$ = 6.8 Hz, 2H, OCH_2), 3.69 (t, $^3J_{HH}$ = 5.2 Hz, 2H, OCH_2), 4.29 (t, $^3J_{HH}$ = 4.8 Hz, 2H, CO_2CH_2), 4.74 (d, $^3J_{HH}$ = 5.6 Hz, 2H, NCH_2), 7.17 (d, $^3J_{HH}$ = 8.4 Hz, 2H, Ph), 7.34 (d, $^3J_{HH}$ = 8.4 Hz, 2H, Ph), 10.33 (s, 1H, NH).

Data for **I-3**: yield, 90.0%; mp, 69–70 °C; ^{1}H NMR ($CDCl_3$), δ 1.21 (t, $^3J_{HH}$ = 7.2 Hz, 3H, CH_3), 2.69 (s, 3H, SCH_3), 3.57 (q, $^3J_{HH}$ = 6.9 Hz, 2H, OCH_2), 3.69 (t, $^3J_{HH}$ = 5.1 Hz, 2H, OCH_2), 4.30 (t, $^3J_{HH}$ = 5.1 Hz, 2H, CO_2CH_2), 4.78 (d, $^3J_{HH}$ = 6.0 Hz, 2H, NCH_2), 7.36 (d, $^3J_{HH}$ = 8.4 Hz, 1H, Py), 7.55 (dd, $^3J_{HH}$ = 8.4 Hz, $^4J_{HH}$ =2.4 Hz, 1H, Py), 8.33 (d, $^4J_{HH}$ = 2.4 Hz, 1H, Py), 10.35 (s, 1H, NH).

Data for **I-4**: yield, 60.0%; mp, 79–80 °C; ^{1}H NMR ($CDCl_3$), δ 1.21 (t, $^3J_{HH}$ = 6.8 Hz, 3H, CH_3), 2.69 (s, 3H, SCH_3), 3.57 (q, $^3J_{HH}$ = 6.8 Hz, 2H, OCH_2), 3.70 (t, $^3J_{HH}$ = 4.8 Hz, 2H, OCH_2), 4.30 (t, $^3J_{HH}$ = 5.1 Hz, 2H, CO_2CH_2), 4.76 (d, $^3J_{HH}$ = 6.3 Hz, 2H, NCH_2), 7.43–7.53 (m, 2H, Py), 8.31 (d, $^4J_{HH}$ = 2.4 Hz, 1H, Py), 10.34 (s, H, NH). Anal. Calcd for $C_{15}H_{18}BrN_3O_3S$ (%): C, 45.01; H, 4.53; N, 10.50. Found: C, 44.96; H, 4.57; N, 10.41.

Data for **I-5**: yield, 90.1%; mp, 77–79 °C; ^{1}H NMR ($CDCl_3$), δ 1.21 (t, $^3J_{HH}$ = 6.9 Hz, 3H, CH_3), 1.28 (t, $^3J_{HH}$ = 7.8 Hz, 3H, CH_3), 2.64 (q, $^3J_{HH}$ = 7.8 Hz, 2H, $CH_2C{\equiv}C$), 3.57 (q, $^3J_{HH}$ = 6.9 Hz, 2H, OCH_2), 3.69 (t, $^3J_{HH}$ = 5.4 Hz, 2H, OCH_2), 4.28 (t, $^3J_{HH}$ = 5.1 Hz, 2H, CO_2CH_2), 4.54 (d, $^3J_{HH}$ = 6.0 Hz, 2H, NCH_2), 7.44–7.55 (m, 2H, Py), 8.31 (d, $^4J_{HH}$ = 2.1 Hz, 1H, Py), 10.18 (s, 1H, NH). Anal. Calcd for $C_{16}H_{20}BrN_3O_3$ (%): C, 50.27; H, 5.27; N, 10.99. Found: C, 50.29; H, 5.23; N, 10.95.

Data for **I-6**: yield, 75.0%; mp, 121–122 °C; ^{1}H NMR ($CDCl_3$), δ 1.21 (t, $^3J_{HH}$ = 6.9 Hz, 3H, CH_3), 1.39 (d, $^3J_{HH}$ = 7.2 Hz, 6H, $C(CH_3)_2$), 3.10–3.19 (m, 1H, CH), 3.58 (q, $^3J_{HH}$ = 6.9 Hz, 2H, OCH_2), 3.69 (t, $^3J_{HH}$ = 5.1 Hz, 2H, OCH_2), 4.28 (t, $^3J_{HH}$ = 5.1 Hz, 2H, CO_2CH_2), 4.60 (d, $^3J_{HH}$ = 6.0 Hz, 2H, NCH_2), 7.45–7.55 (m, 2H, Py), 8.31 (d, $^4J_{HH}$ = 2.4 Hz, 1H, Py), 10.57 (s, 1H, NH). Anal. Calcd for $C_{17}H_{22}BrN_3O_3$ (%): C, 51.52; H, 5.60; N, 10.60. Found: C, 51.46; H, 5.61; N, 10.50.

Data for **I-7**: yield, 52.7%; mp, 95–97 °C; ^{1}H NMR ($CDCl_3$), δ 1.22 (t, $^3J_{HH}$ = 6.9 Hz, 3H, CH_3), 2.71 (s, 3H, SCH_3), 3.11 (s, 6H, $N(CH_3)_2$), 3.58 (q, $^3J_{HH}$ = 6.9 Hz, 2H, OCH_2), 3.70 (t, $^3J_{HH}$ = 5.4 Hz, 2H, OCH_2), 4.29 (t, $^3J_{HH}$ = 5.1 Hz, 2H, CO_2CH_2), 4.63 (d, $^3J_{HH}$ = 5.7 Hz, 2H, NCH_2), 6.53 (d, $^3J_{HH}$ = 9.0 Hz, 1H, Py), 7.35–7.39 (m, 1H, Py), 8.10 (d, $^4J_{HH}$ = 2.1 Hz, 1H, Py), 10.19 (s, 1H, NH). Anal. Calcd for $C_{17}H_{24}N_4O_3S$ (%): C, 56.02; H, 6.64; N, 15.37. Found: C, 56.27; H, 6.52; N, 15.27.

Data for **I-8**: yield, 44.0%; mp, 73–74 °C; ^{1}H NMR ($CDCl_3$), δ 1.20 (t, $^3J_{HH}$ = 7.2 Hz, 3H, CH_3), 1.41 (d, $^3J_{HH}$ = 7.2 Hz, 6H, $C(CH_3)_2$), 3.00 (s, 6H, $N(CH_3)_2$), 3.20–3.29 (m, 1H, CH), 3.57 (q, $^3J_{HH}$ = 7.2 Hz, 2H, OCH_2), 3.68 (t, $^3J_{HH}$ = 5.1 Hz, 2H, OCH_2), 4.25 (t, $^3J_{HH}$ = 5.4 Hz, 2H, CO_2CH_2), 4.45 (d, $^3J_{HH}$ = 5.7 Hz, 2H, NCH_2), 6.52 (d, $^3J_{HH}$ = 8.7 Hz, 1H, Py), 7.33–7.36 (m, 1H, Py), 8.06 (d, $^4J_{HH}$ = 2.1 Hz, 1H, Py), 10.45 (s, 1H, NH). Anal. Calcd for $C_{19}H_{28}N_4O_3$ (%): C, 63.31; H, 7.83; N, 15.54. Found: C, 63.21; H, 7.71; N, 15.78.

Data for **I-9**: yield, 94.0%; mp, 54–56 °C; ^{1}H NMR ($CDCl_3$), δ 1.21 (t, $^3J_{HH}$ = 6.9 Hz, 3H, CH_3), 2.70 (s, 3H, SCH_3), 3.57 (q, $^3J_{HH}$ = 7.8 Hz, 2H, OCH_2), 3.69 (t, $^3J_{HH}$ = 4.8 Hz, 2H, OCH_2), 4.29 (t, $^3J_{HH}$ = 5.4 Hz, 2H, CO_2CH_2), 4.72–4.80 (m, 4H, CF_3CH_2, NCH_2), 6.89 (d, $^3J_{HH}$ = 8.4 Hz, 1H, Py), 7.54–7.58 (m, 1H, Py), 8.07 (d, $^4J_{HH}$ = 2.4 Hz, 1H, Py), 10.29 (s, 1H, NH). Anal. Calcd for $C_{17}H_{20}F_3N_3O_4S$ (%): C, 48.68; H, 4.81; N, 10.02. Found: C, 48.70; H, 4.96; N, 9.95.

Data for **I-11**: yield, 98.0%; mp, 79–81 °C; ^{1}H NMR ($CDCl_3$), δ 1.21 (t, $^3J_{HH}$ = 6.9 Hz, 3H, CH_3), 2.73 (s, 3H, SCH_3), 3.57 (q, $^3J_{HH}$ = 6.9 Hz, 2H, OCH_2), 3.69 (t, $^3J_{HH}$ = 5.1 Hz, 2H, OCH_2), 4.30 (t, $^3J_{HH}$ = 5.1 Hz, 2H, CO_2CH_2), 4.91 (d, $^3J_{HH}$ = 7.2 Hz, 2H, NCH_2), 7.48 (s, 1H, thiazole), 10.31 (s, 1H, NH). Anal. Calcd for $C_{13}H_{16}BrN_3O_3S_2$ (%): C, 38.43; H, 3.97; N, 10.34. Found: C, 38.19; H, 3.96; N, 10.31.

Data for **I-12**: yield, 80.0%; mp, 76–78 °C; ^{1}H NMR ($CDCl_3$), δ 1.21 (t, $^3J_{HH}$ = 6.9 Hz, 3H, CH_3), 1.43 (d, $^3J_{HH}$ = 6.9 Hz, 6H, $C(CH_3)_2$), 3.14–3.21 (m, 1H, CH), 3.58 (q, $^3J_{HH}$ = 6.9 Hz, 2H, OCH_2), 3.69 (t, $^3J_{HH}$ = 5.1 Hz, 2H, CH_2O), 4.29 (t, $^3J_{HH}$ = 5.1 Hz, 2H, CO_2CH_2), 4.74 (d, $^3J_{HH}$ = 6.0 Hz, 2H, NCH_2), 7.47 (s, 1H, thiazole), 10.54 (s, 1H, NH). Anal. Calcd for $C_{15}H_{20}BrN_3O_3S$ (%): C, 44.78; H, 5.01; N, 10.44. Found: C, 44.50; H, 5.03; N, 10.28.

Data for **I-13**: yield, 87.5%; yellow oil; ^{1}H NMR ($CDCl_3$), δ 1.21 (t, $^3J_{HH}$ = 6.9 Hz, 3H, CH_3), 1.43 (t, $^3J_{HH}$ = 7.2 Hz, 3H, CH_3), 2.72 (s, 3H, SCH_3), 3.57 (q, $^3J_{HH}$ = 6.9 Hz, 2H, OCH_2), 3.69 (t, $^3J_{HH}$ = 5.1 Hz, 2H, CH_2O), 4.29 (t, $^3J_{HH}$ = 5.1 Hz, 2H, CO_2CH_2), 4.44 (q, $^3J_{HH}$ = 7.2 Hz, 2H, OCH_2), 4.78 (d, $^3J_{HH}$ = 6.0 Hz, 2H, NCH_2), 7.02 (s, 1H, thiazole), 10.21 (s, 1H, NH). HRMS, *m/z* 394.0864. Calcd for $C_{15}H_{21}N_3O_4S_2$ + Na: 394.0866.

Data for **I-14**: yield, 56.3; yellow oil; ^{1}H NMR ($CDCl_3$), δ 1.02 (t, $^3J_{HH}$ = 6.9 Hz, 3H, CH_3), 1.21 (t, $^3J_{HH}$ = 7.0 Hz, 3H, CH_3), 1.43 (d, $^3J_{HH}$ = 6.9 Hz, 6H, $C(CH_3)_2$), 3.18–3.27 (m, 1H, CH), 3.57 (q, $^3J_{HH}$ = 6.9 Hz, 2H, OCH_2), 3.69 (t, $^3J_{HH}$ = 5.1 Hz, 2H, OCH_2), 4.29 (t, $^3J_{HH}$ = 5.1 Hz, 2H, CO_2CH_2), 4.44 (q, $^3J_{HH}$ = 7.0 Hz, 2H, OCH_2), 4.78 (d, $^3J_{HH}$ = 6.0 Hz, 2H, NCH_2), 7.02 (s, 1H, thiazole), 10.21 (s, 1H, NH). HRMS, *m/z* 390.1457. Calcd for $C_{17}H_{25}N_3O_4S$ + Na: 390.1458.

Data for **I-15**: yield, 85.0%; yellow oil; ^{1}H NMR ($CDCl_3$), δ 1.02 (t, $^3J_{HH}$ = 6.9 Hz, 3H, CH_3), 1.21 (t, $^3J_{HH}$ = 6.9 Hz, 3H, CH_3), 1.76–1.88 (m, 2H, CCH_2C), 2.72 (s, 3H, SCH_3), 3.57 (q, $^3J_{HH}$ = 6.9 Hz, 2H, OCH_2), 3.69 (t, $^3J_{HH}$ = 5.1 Hz, 2H, OCH_2), 4.27–4.36 (m, 4H, OCH_2, CO_2CH_2), 4.78 (d, $^3J_{HH}$ = 6.0 Hz, 2H, NCH_2), 7.01 (s, 1H, thiazole), 10.21 (s, 1H, NH). HRMS, *m/z* 408.1018. Calcd for $C_{16}H_{23}N_3O_4S_2$ + Na: 408.1022.

Data for **I-16**: yield, 70.0%; yellow oil; ^{1}H NMR ($CDCl_3$), δ 1.02 (t, $^3J_{HH}$ = 6.9 Hz, 3H, CH_3), 1.21 (t, $^3J_{HH}$ = 7.2 Hz, 3H, CH_3), 1.43 (d, $^3J_{HH}$ = 6.9 Hz, 6H, $C(CH_3)_2$), 1.76–1.88 (m, 2H, CCH_2C), 3.18–3.27

Chart 1. Framework of Molecular Structures

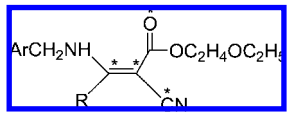

(m, 1H, CH), 3.58 (q, $^3J_{HH}$ = 6.9 Hz, 2H, OCH_2), 3.69 (t, $^3J_{HH}$ = 5.1 Hz, 2H, OCH_2), 4.27 (t, $^3J_{HH}$ = 5.1 Hz, 2H, CO_2CH_2), 4.34 (t, $^3J_{HH}$ = 7.2 Hz, 2H, OCH_2), 4.61 (d, $^3J_{HH}$ = 6.0 Hz, 2H, NCH_2), 7.00 (s, 1H, thiazole), 10.43 (s, 1H, NH). HRMS, *m/z* 404.1612. Calcd for $C_{18}H_{27}N_3O_4S$ + Na: 404.1614.

Data for **I-17**: yield, 89.0%; yellow oil; ^{1}H NMR ($CDCl_3$), δ 1.21 (t, $^3J_{HH}$ = 6.9 Hz, 3H, CH_3), 1.40 (d, $^3J_{HH}$ = 7.2 Hz, 6H, $C(CH_3)_2$), 2.72 (s, 3H, SCH_3), 3.57 (q, $^3J_{HH}$ = 6.9 Hz, 2H, OCH_2), 3.68 (t, $^3J_{HH}$ = 5.1 Hz, 2H, OCH_2), 4.29 (t, $^3J_{HH}$ = 5.1 Hz, 2H, CO_2CH_2), 4.77 (d, $^3J_{HH}$ = 6.0 Hz, 2H, NCH_2), 5.12–5.20 (m, 1H, CHO), 7.00 (s, 1H, thiazole), 10.20 (s, 1H, NH). HRMS, *m/z* 408.1023. Calcd for $C_{16}H_{23}N_3O_4S_2$ + Na: 408.1022.

Data for **I-18**: yield, 67.0%; yellow oil; ^{1}H NMR ($CDCl_3$), δ 1.21 (t, $^3J_{HH}$ = 6.9 Hz, 3H, CH_3), 1.39–1.44 (m, 12H, $C(CH_3)_2$, $OC(CH_3)_2$), 3.18–3.27 (m, 1H, CH), 3.58 (q, $^3J_{HH}$ = 6.9 Hz, 2H, OCH_2), 3.69 (t, $^3J_{HH}$ = 5.1 Hz, 2H, CH_2O), 4.27 (t, $^3J_{HH}$ = 5.1 Hz, 2H, CO_2CH_2), 4.60 (d, $^3J_{HH}$ = 6.0 Hz, 2H, NCH_2), 5.12–5.20 (m, 1H, CHO), 6.99 (s, 1H, thiazole), 10.42 (s, 1H, NH). HRMS, *m/z* 404.1613. Calcd for $C_{18}H_{27}N_3O_4S$ + Na: 404.1614.

Data for **I-19**: yield, 90.6%; yellow oil; ^{1}H NMR ($CDCl_3$), δ 1.20 (t, $^3J_{HH}$ = 6.9 Hz, 3H, CH_3), 2.73 (s, 3H, SCH_3), 3.57 (q, $^3J_{HH}$ = 6.9 Hz, 2H, OCH_2), 3.69 (t, $^3J_{HH}$ = 5.1 Hz, 2H, CH_2O), 4.27 (t, $^3J_{HH}$ = 5.1 Hz, 2H, CO_2CH_2), 4.75–4.83 (m, 4H, NCH_2, CF_3CH_2O), 7.04 (s, 1H, thiazole), 10.24 (s, 1H, NH). HRMS, *m/z* 448.0580. Calcd for $C_{15}H_{18}F_3N_3O_4S_2$ + Na: 448.0583.

Data for **I-20**: yield 92.1%; yellow oil; ^{1}H NMR ($CDCl_3$), δ 1.21 (t, $^3J_{HH}$ = 6.9 Hz, 3H, CH_3), 1.43 (d, $^3J_{HH}$ = 7.2 Hz, 6H, $C(CH_3)_2$), 3.17–3.27 (m, 1H, CH), 3.58 (q, $^3J_{HH}$ = 6.9 Hz, 2H, OCH_2), 3.69 (t, $^3J_{HH}$ = 5.1 Hz, 2H, OCH_2), 4.28 (t, $^3J_{HH}$ = 5.1 Hz, 2H, CO_2CH_2), 4.63 (d, $^3J_{HH}$ = 6.0 Hz, 2H, NCH_2), 4.80 (q, $^3J_{HF}$ = 8.1 Hz, 2H, CF_3CH_2), 7.03 (s, 1H, thiazole), 10.46 (s, 1H, NH). HRMS, *m/z* 444.1170. Calcd for $C_{17}H_{22}F_3N_3O_4S$ + Na: 444.1175.

Data for **I-21**: yield, 69.0%; mp, 103–104 °C; ^{1}H NMR ($CDCl_3$), δ 1.21 (t, $^3J_{HH}$ = 7.0 Hz, 3H, CH_3), 2.71 (s, 3H, SCH_3), 3.58 (q, $^3J_{HH}$ = 7.0 Hz, 2H, OCH_2), 3.71 (t, $^3J_{HH}$ = 5.1 Hz, 2H, OCH_2), 4.32 (t, $^3J_{HH}$ = 5.1 Hz, 2H, CO_2CH_2), 5.12 (d, $^3J_{HH}$ = 6.0 Hz, 2H, NCH_2), 7.39 (d, $^3J_{HH}$ = 9.0 Hz, 1H, pyridazine), 7.56 (d, $^3J_{HH}$ = 9.0 Hz, 1H, pyridazine), 10.64 (s, 1H, NH). Anal. Calcd for $C_{14}H_{17}ClN_4O_3S$ (%): C, 47.12; H, 4.80; N, 15.70. Found: C, 47.13; H, 4.86; N, 15.89.

Data for **I-22**: yield, 68.0%; mp, 116–117 °C; ^{1}H NMR ($CDCl_3$), δ 1.20 (t, $^3J_{HH}$ = 7.0 Hz, 2H, CH_3), 1.36 (d, $^3J_{HH}$ = 7.2 Hz, 6H, $C(CH_3)_2$), 3.20 (m, 1H, CH), 3.57 (q, $^3J_{HH}$ = 6.8 Hz, 2H, OCH_2), 3.70 (t, $^3J_{HH}$ = 4.8 Hz, 2H, OCH_2), 4.30 (t, $^3J_{HH}$ = 4.8 Hz, 2H, CO_2CH_2), 4.94 (d, $^3J_{HH}$ = 6.0 Hz, 2H, NCH_2), 7.44 (d, $^3J_{HH}$ = 8.8 Hz, 1H, pyridazine), 7.59 (d, $^3J_{HH}$ = 8.8 Hz, 1H, pyridazine), 10.88 (s, 1H, NH). Anal. Calculated for $C_{16}H_{21}ClN_4O_3$ (%): C, 54.47; H, 6.00; N, 15.88. Found: C, 54.63; H, 6.12; N, 16.06.

Data for **I-23**: yield, 58.0%; mp, 72–73 °C; ^{1}H NMR ($CDCl_3$), δ 1.21 (t, $^3J_{HH}$ = 6.9 Hz, 3H, CH_3), 1.45 (t, $^3J_{HH}$ = 7.0 Hz, 3H, CH_3), 2.70 (s, 3H, SCH_3), 3.57 (q, $^3J_{HH}$ = 6.9 Hz, 2H, OCH_2), 3.70 (t, $^3J_{HH}$ = 5.2 Hz, 2H, OCH_2), 4.31 (t, $^3J_{HH}$ = 5.1 Hz, 2H, CO_2CH_2), 4.59 (q, $^3J_{HH}$ = 7.1 Hz, 2H, OCH_2), 4.50 (d, $^3J_{HH}$ = 6.0 Hz, 2H, NCH_2), 6.97 (d, $^3J_{HH}$ = 9.0 Hz, 1H, pyridazine), 7.28 (d, $^3J_{HH}$ = 9.0 Hz, 1H, pyridazine), 10.64 (s, 1H, NH). Anal. Calcd for $C_{16}H_{22}N_4O_4S$ (%): C, 52.44; H, 6.05; N, 15.29. Found: C, 52.23; H, 5.87; N, 14.83.

Data for **I-24**: yield, 44.0%; yellow oil; ^{1}H NMR ($CDCl_3$), δ 1.21 (t, $^3J_{HH}$ = 7.0 Hz, 3H, CH_3), 1.37 (d, $^3J_{HH}$ = 7.2 Hz, 6H, $C(CH_3)_2$), 1.45 (t, $^3J_{HH}$ = 7.2 Hz, 3H, CH_3), 3.26 (m, 1H, CH), 3.58 (q, $^3J_{HH}$ = 7.0 Hz, 2H, OCH_2), 3.70 (t, $^3J_{HH}$ = 5.1 Hz, 2H, OCH_2), 4.30 (t, $^3J_{HH}$ = 5.1 Hz, 2H, CO_2CH_2), 4.59 (q, $^3J_{HH}$ = 7.2 Hz, 2H, OCH_2), 4.82 (d, $^3J_{HH}$ = 6.0 Hz, 2H, NCH_2), 6.99 (d, $^3J_{HH}$ = 9.0 Hz, 1H, pyridazine), 7.31 (d, $^3J_{HH}$ = 9.0 Hz, 1H, pyridazine), 10.85 (s, 1H, NH). Anal. Calcd for $C_{18}H_{26}N_4O_4$ (%): C, 59.65; H, 7.23; N, 15.46. Found: C, 59.80; H, 7.40; N, 15.21.

Scheme 1

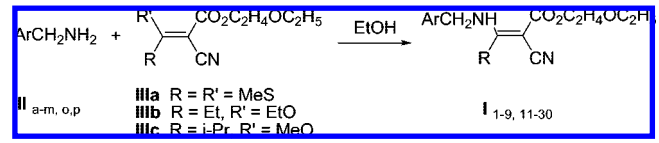

Scheme 2

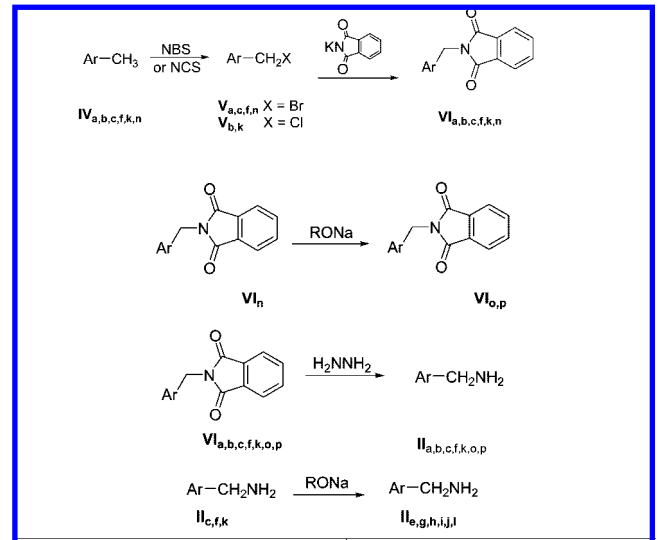

II, IV, V, VI	Ar	II, IV, V, VI	Ar
a	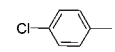	i	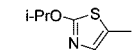
b	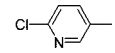	j	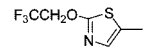
c	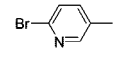	k	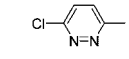
e	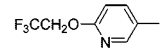	l	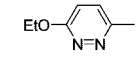
f	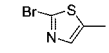	n	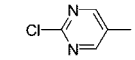
g	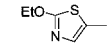	o	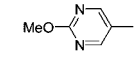
h	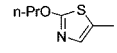	p	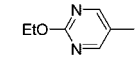

Data for **I-25**: yield, 43.0%; yellow oil; ^{1}H NMR ($CDCl_3$), δ 1.21 (t, $^3J_{HH}$ = 6.9 Hz, 3H, CH_3), 2.70 (s, 3H, SCH_3), 3.57 (q, $^3J_{HH}$ = 7.0 Hz, 2H, OCH_2), 3.64 (t, $^3J_{HH}$ = 4.9 Hz, 4H, $N(CH_2)_2$), 3.69 (t, $^3J_{HH}$ = 5.1 Hz, 2H, OCH_2), 3.85 (t, $^3J_{HH}$ = 4.8 Hz, 4H, $O(CH_2)_2$), 4.30 (t, $^3J_{HH}$ = 5.1 Hz, 2H, CO_2CH_2), 4.96 (d, $^3J_{HH}$ = 5.7 Hz, 2H, NCH_2), 6.90 (d, $^3J_{HH}$ = 9.0 Hz, 1H, pyridazine), 7.17 (d, $^3J_{HH}$ = 9.0 Hz, 1H, pyridazine), 10.57 (s, 1H, NH). Anal. Calcd for $C_{18}H_{25}N_5O_4S$ (%): C, 53.06; H, 6.18; N, 17.19. Found: C, 52.51; H, 6.82; N, 17.37.

Data for **I-26**: yield, 31.0%; yellow oil; ^{1}H NMR ($CDCl_3$), δ 1.21 (t, $^3J_{HH}$ = 7.0 Hz, 3H, CH_3), 1.37 (d, $^3J_{HH}$ = 7.2 Hz, 6H, $C(CH_3)_2$), 3.29 (m, 1H, CH), 3.58 (q, $^3J_{HH}$ = 7.0 Hz, 2H, OCH_2), 3.64 (t, $^3J_{HH}$ = 4.9 Hz, 4H, $N(CH_2)_2$), 3.70 (t, $^3J_{HH}$ = 5.2 Hz, 2H, OCH_2), 3.85 (t, $^3J_{HH}$ = 4.8 Hz, 4H, $O(CH_2)_2$), 4.29 (t, $^3J_{HH}$ = 5.2 Hz, 2H, CO_2CH_2), 4.78 (d, $^3J_{HH}$ = 5.7 Hz, 2H, NCH_2), 6.92 (d, $^3J_{HH}$ = 9.3 Hz, 1H, pyridazine), 7.20 (d, $^3J_{HH}$ = 9.3 Hz, 1H, pyridazine), 10.78 (s, 1H, NH). Anal. Calcd for $C_{20}H_{29}N_5O_4$ (%): C, 59.54; H, 7.24; N, 17.36. Found: C, 59.14; H, 7.43; N, 17.30.

Data for **I-27**: yield, 68.0%; mp, 75–76 °C; ^{1}H NMR ($CDCl_3$), δ 1.21 (t, $^3J_{HH}$ = 7.2 Hz, 3H, CH_3), 2.72 (s, 3H, SCH_3), 3.57 (q, $^3J_{HH}$ =

Scheme 3

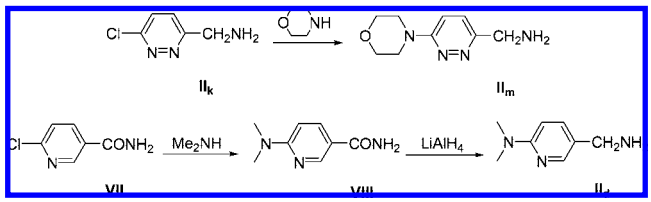

7.2 Hz, 2H, OCH_2), 4.05 (s, 3H, OCH_3), 3.69 (t, $^3J_{HH}$ = 5.1 Hz, 2H, OCH_2), 4.30 (t, $^3J_{HH}$ = 5.1 Hz, 2H, CO_2CH_2), 4.73 (d, $^3J_{HH}$ = 5.7 Hz, 2H, NCH_2), 8.48 (s, 2H, pyrimidine), 10.32 (s, 1H, NH). Anal. Calcd for $C_{15}H_{20}N_4O_4S$ (%): C, 51.12; H, 5.72; N, 15.90. Found: C, 51.19; H, 5.44; N, 15.70.

Data for **I-28**: yield, 43.2%; mp, 52–54 °C; ^{1}H NMR ($CDCl_3$), δ 1.21 (t, $^3J_{HH}$ = 7.2 Hz, 3H, CH_3), 1.31 (t, $^3J_{HH}$ = 7.8 Hz, 3H, CH_3), 2.69 (q, $^3J_{HH}$ = 7.8 Hz, 2H, CCH_2), 3.57 (q, $^3J_{HH}$ = 7.2 Hz, 2H, OCH_2), 3.68 (t, $^3J_{HH}$ = 5.1 Hz, 2H, OCH_2), 4.04 (s, 3H, OCH_3), 4.28 (t, $^3J_{HH}$ = 5.1 Hz, 2H, CO_2CH_2), 4.51 (d, $^3J_{HH}$ = 5.7 Hz, 2H, NCH_2), 8.47 (s, 2H, pyrimidine), 10.10 (s, 1H, NH). Anal. Calcd for $C_{16}H_{22}N_4O_4$ (%): C, 57.47; H, 6.63; N, 16.76. Found: C, 57.31; H, 6.75; N, 16.63.

Data for **I-29**: yield, 82.6%; mp, 108–110 °C; ^{1}H NMR ($CDCl_3$), δ 1.21 (t, $^3J_{HH}$ = 7.2 Hz, 3H, CH_3), 1.43 (d, $^3J_{HH}$ = 6.9 Hz, 6H, $C(CH_3)_2$), 3.57 (q, $^3J_{HH}$ = 7.2 Hz, 2H, OCH_2), 3.18–3.22 (m, 1H, CH), 3.69 (t, $^3J_{HH}$ = 5.1 Hz, 2H, OCH_2), 4.04 (s, 3H, OCH_3), 4.27 (t, $^3J_{HH}$ = 5.1 Hz, 2H, CO_2CH_2), 4.56 (d, $^3J_{HH}$ = 5.4 Hz, 2H, NCH_2), 8.47 (s, 2H, pyrimidine), 10.49 (s, 1H, NH). Anal. Calcd for $C_{17}H_{24}N_4O_4$ (%): C, 58.61; H, 6.94; N, 16.08. Found: C, 58.58; H, 6.91; N, 15.97.

Data for **I-30**: yield, 64.6%; mp, 90–92 °C; ^{1}H NMR ($CDCl_3$), δ 1.21 (t, $^3J_{HH}$ = 7.2 Hz, 3H, CH_3), 1.44 (t, $^3J_{HH}$ = 7.2 Hz, 3H, CH_3), 2.72 (s, 3H, SCH_3), 3.57 (q, $^3J_{HH}$ = 7.2 Hz, 2H, OCH_2), 3.69 (t, $^3J_{HH}$ = 7.2 Hz, 2H, OCH_2), 4.29 (t, $^3J_{HH}$ = 5.1 Hz, 2H, CO_2CH_2), 4.44 (q, $^3J_{HH}$ = 7.2 Hz, 2H, OCH_2), 4.72 (d, $^3J_{HH}$ = 5.7 Hz, 2H, NCH_2), 8.45 (s, 2H, pyrimidine), 10.30 (s, 1H, NH). Anal. Calcd for $C_{16}H_{22}N_4O_4S$ (%): C, 52.44; H, 6.05; N, 15.29. Found: C, 52.32; H, 6.04; N, 15.21.

Crystal Structure Determination. The crystal structure of the compound **I-11** was determined, and X-ray intensity data were recorded on a Bruker SMART 1000 CCD diffraction meter using graphite monochromated Mo Kα radiation (λ = 0.71073 Å). In the range of $2.05° \le \theta \le 26.36°$, 2312 independent reflections were obtained. All calculations were refined anisotropically. All hydrogen atoms were located from a difference Fourier map and were placed at calculated positions and were included in the refinements in the riding mode with isotropic thermal parameters. Final R and R_w values were 0.0387 and 0.0786, respectively $\{\omega = 1/[\sigma^2 (F) + 99.0000 F^2]\}$, and S = 1.024.

Biological Tests. *In Vivo Herbicidal Activity.* Two dicotyledon crops, rape (*Brassica napus* L.) and amaranth pigweed (*Amaranthus retroflexus*), and two monocotyledon crops, alfalfa (*Medicago sativa* L.) and hairy crabgrass (*Digitaria sanguinalis* L. Scop.), were used to test the herbicidal activities of compounds **I-1** to **I-30** using a previously reported procedure (*10*).

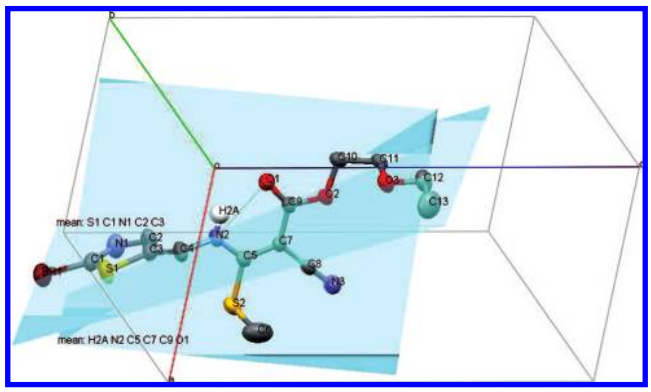

Figure 1. Crystal of compound **I-11**. Hydrogen atoms except H2A are omitted for clarity.

Table 2. Herbicidal Activities of Compounds **I** (1.5 kg/ha, Percent Inhibition)

	postemergence treatment				preemergence treatment			
		amaranth		hairy		amaranth		hairy
compd	rape	pigweed	alfalfa	crabgrass	rape	pigweed	alfalfa	crabgrass
I-1	100	100	68.9	46.4	4.4	40.5	0	12.9
I-2	100	100	12.9	31.2	24.9	59.4	0	24.8
I-3	100	100	41.3	89.9	68.9	13.7	1.5	18.6
I-4	100	100	59.9	60.0	23.9	91.9	12.0	0
I-5	100	100	77.8	95.2	71.9	21.6	28.8	18.8
I-6	100	97.8	32.1	42.4	68.7	48.6	0	16.8
I-7	100	80.9	51.6	45.6	37.4	13.5	0	28.7
I-8	100	100	58.3	88.0	29.3	75.7	27.9	52.5
I-9	100	100	54.2	100	10.0	0	0	0
I-10	100	100	37.1	45.6	70.3	67.6	15.7	28.7
I-11	100	88.0	26.8	36.0	28.7	29.7	8.2	8.9
I-12	100	100	30.8	48.0	82.2	18.9	1.7	3.0
I-13	100	100	62.6	51.2	23.3	43.2	14.8	44.6
I-14	100	100	41.4	51.2	48.7	37.8	5.4	0
I-15	100	100	57.3	49.6	0	27.0	17.6	0
I-16	100	100	48.7	52.8	9.8	27.0	0	6.9
I-17	100	100	53.6	54.4	26.0	40.5	4.5	14.8
I-18	100	100	43.4	60.8	51.4	100	1.7	6.9
I-19	100	98.7	60.9	47.2	65.4	43.2	1.7	8.9
I-20	100	100	53.3	95.2	71.9	51.0	0	34.6
I-21	81.0	21.8	27.8	28.8	12.5	43.2	0	0
I-22	100	91.6	31.4	48.0	59.5	27.0	4.5	10.9
I-23	64.6	32.9	24.2	0.8	0	56.8	0	0
I-24	100	70.2	50.7	57.6	44.9	54.0	0	26.7
I-25	18.1	24.0	32.8	2.4	10.9	13.5	10.1	6.9
I-26	85.4	19.1	15.2	13.6	49.8	5.4	2.6	22.8
I-27	28.8	15.5	45.1	2.2	42.4	58.1	42.8	26.0
I-28	63.7	20.7	26.0	2.2	51.5	34.6	29.4	36.0
I-29	19.4	3.4	74.0	52.2	0	22.2	57.1	46.2
I-30	16.1	26.4	40.8	8.7	0	15.9	31.1	12.5
I-31[a]	47.5	37.8	23.4	0	0	9.5	21.8	35.7
I-32[a]	97.2	100	60.5	100	80.0	3.2	20.3	40.0
I-33[a]	88.2	37.8	41.3	57.6	0	12.6	2.3	0
I-34[a]	51.9	27.4	13.2	0	0	22.1	10.5	33.6

[a] The data of **I-31** to **I-34** were taken from published work (*10*).

In Vitro Measurement of the Hill Reaction. Hill reaction activity was measured as terms of photoreduction of 2,6-dichlorophenolindophenol (DCPIP) mainly as described by Holt and French (*17*). Preparation of functional chloroplasts and the Hill reaction system were modified suitably.

Chloroplasts were isolated from fresh spinach (*Spinacea oleracea* L.) leaves. Plant material was homogenized in ice-cold extraction buffer (pH 7.8) containing 0.4 M sucrose, 10 mM NaCl, and 50 mM Tris-HCl. The homogenate was filtered through surgical gauze, and the filtrate was then centrifuged at 4 °C for 3 min at 120*g*. The supernatant was collected and recentrifuged for 5 min at 1000*g*. Pelleted chloroplasts were finally resuspended in the same buffer, and the chloroplast suspension was kept on ice and away from bright light before Hill reaction measurement.

The rate of photosynthetic electron transport was measured by following light-driven DCPIP reduction. Chloroplast suspension was appropriately diluted before use. The Hill reaction mixture (3 mL) contained the following components: 2.5 mL of reacting buffer (350 mM NaCl, 10 mM Tris-HC1, pH 7.8), 0.35 mL of 0.3 mM DCPIP, and 0.15 mL of chloroplast suspension. The assay was initiated by exposure to light (360 μmol m^{-2} s^{-1}) for 2 min, and the rate of DCPIP reduction was measured against an exact blank at 620 nm. The effect of compounds upon the Hill reaction was evaluated in parallel assays in which the compounds were added to the reaction mixture to concentrations ranging from 0.01 mg/L to 0.3 mg/mL. Each dose had at least triplicate samples. The concentrations causing 50% inhibition (IC_{50}) of in vitro activity were estimated utilizing the linear regression equation of activity values plotted against the logarithm of inhibitor concentration.

Table 3. Herbicidal Activities of Compounds **I** (Percent Inhibition)

		postemergence treatment				postemergence treatment		
compd	dose (kg/ha)	rape	amaranth pigweed	hairy crabgrass	compd	dose (kg/ha)	rape	amaranth pigweed	hairy crabgrass
I-1	750	100	100			375	45.4	43.5	
	375	100	92.3						
	150	87.7	78.2		**I-12**	750	100	74.2	
	75	40.9	54.5			375	100	56.9	
						150	62.9		
I-2	750	100	100			75	35.3		
	375	100	95.2						
	150	6.6	26.7		**I-13**	750	93.1	80.9	
	75	0	17.8			375	77.3	70.3	
I-3	750	100	100		**I-14**	750	100	63.6	
	375	100	92.3			375	94.0	36.8	
	150	73.8	73.3						
	75	55.7	48.0		**I-15**	750	98.5	66.5	
						375	92.5	42.6	
I-4	750	100	100						
	375	100	83.7		**I-16**	750	100	65.6	
	150	58.4				375	100	48.3	
	75	40.0				150	57.1		
						75	22.3		
I-5	750	96.4	100	82.8					
	375	94.6	100	69.4	**I-17**	750	79.1	61.7	
	150	44.8	83.3			375	71.9	40.7	
	75	8.0	74.0						
					I-18	750	100	63.6	
I-6	750	100	84.7			375	100	63.6	
	375	89.0	42.6			150	57.1		
						75	37.1		
I-7	750	91.4	56.9						
	375	44.1	39.7		**I-19**	750	100	73.2	
						375	100	63.6	
I-8	750	100	78.0	96.4		150	56.0		
	375	100	49.3	85.7		75	40.9		
	150	56.7							
	75	41.9			**I-20**	750	100	100	100
						375	100	91.4	94.6
I-9	750	100	85.0	15.1		150	83.3	98.0	11.3
	375	100	61.0	0		75	50.9	76.7	8.0
I-10	750	100	100		**I-22**	750	94.8	70.3	
	375	100	62.7			375	95.7	33.0	
	150	69.4							
	75	63.8			**I-32**[a]	750	70.2	100	67.9
						375	65.0	100	32.1
I-11	750	82.7	72.2						

[a] The data of **I-32** were taken from published work (*10*).

All of the compounds were dissolved in *N*,*N*-methylformamide and then diluted with water, as desired. Controls received similar amounts of solvent.

Structure–Activity Relationships. *Data Sets for 3D-QSAR Analysis.* Molecular modeling was performed using SYBYL 6.91 software (Tripos, Inc.). The structures and biological activities of the 29 compounds used to derive the CoMFA analyses model are listed in **Table 4**. The crystal structure of compound **I-11** was used as a template to build the other molecular structures. Each structure was fully geometry-optimized using a conjugate gradient procedure based on the TRIPOS force field and Gasteiger and Hückel charges. Because these compounds share a common skeleton, four atoms marked with an asterisk (shown in **Chart 1**) were used for rms-fitting onto the corresponding atoms of the template structure.

CoMFA Descriptors. CoMFA steric and electrostatic interaction fields were calculated at each lattice intersection on a regularly spaced grid of 2.0 Å. The grid pattern was generated automatically by the SYBYL/CoMFA routine, and an sp^3 carbon atom with a van der Waals radius of 1.52 Å and a +1.0 charge was used as the probe to calculate the steric (Lennard-Jones 6–12 potential) field energies and electrostatic (Coulombic potential) fields with a distance-dependent dielectric at each lattice point. Values of the steric and electrostatic fields were truncated at 30.0 kcal/mol. The CoMFA steric and electrostatic fields generated were scaled by the CoMFA-STD method in SYBYL. The electrostatic fields were ignored at the lattice points with maximal steric interactions.

A partial least-squares (PLS) approach was used to derive the 3D-QSAR, in which the CoMFA descriptors were used as independent variables, and pIC_{50} values were used as dependent variables. The cross-validation with the leave-one-out (LOO) option and the SAMPLS program, rather than column filtering, was carried out to obtain the optimal number of components to be used in the final analysis. After the optimal number of components was determined, a non-cross-validated analysis was performed without column filtering. The modeling capability (goodness of fit) was judged by the correlation coefficient squared, r^2, and the prediction capability (goodness of prediction) was indicated by the cross-validated r^2 (q^2).

RESULTS AND DISCUSSION

Synthesis. The title compounds **I** were synthesized from arylmethylamine **II** and alkyoxy- or methylthio-substituted cyanoacrylate **III** with good yields (**Scheme 1**; **Table 1**).

Halo-substituted arylmethylamines **IIa**, **IIb**, **IIc**, **IIf**, and **IIk** were prepared by starting from haloaryl methane **IV**. **IV** was reacted with NBS or NCS in the presence of AIBN and afforded

Table 4. Experimental and Predicted Activities of Compounds **I**

compd	obsd IC_{50} (ppm)	pIC_{50} obsd	pIC_{50} calcd[a]	res
I-1	0.043	7.37	7.04	0.33
I-2	0.026	7.59	7.45	0.14
I-3	0.167	6.78	7.10	−0.32
I-4	0.084	7.08	6.83	0.25
I-5	0.335	6.47	6.48	−0.01
I-6	0.099	7.00	7.13	−0.13
I-7	0.292	6.53	6.33	0.20
I-8	0.086	7.07	7.12	−0.05
I-9	0.048	7.32	7.33	−0.01
I-10	0.161	6.79	6.75	0.04
I-11	0.102	6.99	6.66	0.33
I-12	0.107	6.97	6.82	0.15
I-13	0.115	6.94	6.81	0.13
I-14	0.223	6.65	6.75	−0.10
I-15	0.05	7.30	7.53	−0.23
I-16	0.08	7.10	6.90	0.20
I-17	0.07	7.15	7.46	−0.31
I-18	0.076	7.12	6.98	0.14
I-19	0.055	7.26	7.32	−0.06
I-20	0.074	7.13	7.32	−0.19
I-21	3.99	5.40	5.59	−0.19
I-22	4.3	5.37	5.21	0.16
I-23	12.29	5.04	4.98	0.06
I-27	3.79	5.42	5.44	−0.02
I-30	1.45	5.97	5.71	0.26
I-31	27.92	4.68	4.98	−0.30
I-32	6.874	5.16	5.20	−0.04
I-33	41.4	4.38	4.30	0.08
I-34	6.6	5.18	5.67	−0.49

[a] Calculated using the CoMFA model.

chloromethyl or bromomethyl compounds **V**, and then their reaction with potassium phthalimide gave N-substituted phthalimides **VI**. **VI** was refluxed with hydrazine to afford the corresponding methylamine **II**. Alkoxy-substituted arylmethylamines **IIe**, **IIg**, **IIh**, **IIi**, **IIj**, and **IIl** were prepared from chloroarylmethylamine **IIc**, **IIf**, or **IIk** with sodium alkoxide in alcohol solvent. However, **IIo** and **IIp** were obtained from corresponding phthalimides **VIo** and **VIp**, which were synthesized by refluxing **VIn** with sodium methoxide and ethoxide, respectively (**Scheme 2**).

(6-Morpholinopyridazin-3-yl)methanamine **IIm** was prepared from (6-chloropyridazin-3-yl)methanamine **IIk** with morpholine. 5-(Aminomethyl)-*N*,*N*-dimethylpyridin-2-amine **IId** was prepared by the reduction of *N*,*N*-dimethylpyridine-5-carboxamide **VIII**, which was obtained from 2-chloropyridine-5-carboxamide **VII** (**Scheme 3**).

Most of the intermediates were determined by ^{1}H NMR, and all new title compounds were characterized with ^{1}H NMR and elemental analysis (or HRMS).

Crystal Structure Analysis. Compound **I-11** was recrystallized from ethyl acetate/petroleum ether to give a colorless crystal suitable for X-ray single-crystal diffraction with the following crystallographic parameters: $a = 7.5899(16)$ Å, $b = 21.892(5)$ Å, $c = 9.352(2)$ Å, $\alpha = 90.00°$, $\beta = 106.485(4)°$, $\gamma = 90.00°$, $\mu = 0.092$, $V = 1490.1(6)$ Å^3. The crystal is monoclinic, and in one unit there are four molecules arranged in a pattern of central symmetry.

It can be seen from **Figure 1** that amino and carbonyl are on the same side of the vinyl, and there exists an intramolecular hydrogen bond between the nitrogen atom and the oxygen of the carbonyl. Due to the hydrogen bond, the atoms H2A-N2-C5-C7-C9-O1 are close to planar. This plane and the plane of the thiazole ring (S1-C1-N1-C2-C3) have a dihedral angle of 88.64°; that is, they are nearly perpendicular to each other. The structure was used as the template for studying the 3D-QSAR analysis.

Herbicidal Activity Bioassay. Herbicidal activities of compounds **I-1** to **I-34** are listed in **Table 2**. In postemergence treatment, most of the compounds showed higher herbicidal activities compared to preemergence treatment, and the compounds exhibited higher herbicidal activities against dicotyledon weeds (rape and amaranth pigweed) than against monocotyledon weeds (alfalfa and hairy crabgrass). Benzene-containing compounds (**I-1**, **I-2**), pyridine-containing compounds (**I-3** to **I-9**), and thiazole-containing compounds (**I-10** to **I-20**) gave obviously higher activities than pyridazine (**I-21** to **I-26**), pyrimidine (**I-27** to **I-30**), and tetrahydronfuran and furan (**I-31** to **I-34**) analogues.

Their herbicidal activities at a lower dose revealed the influence of substituent on their reactivity (**Table 3**). 3-Isopropylacrylate compounds **I-1**, **I-8**, **I-12**, **I-16**, and **I-20** exhibited higher activities than 3-methylthio analogues **I-2**, **I-7**, **I-11**, **I-15**, and **I-19**, which indicated the group at this position played an important role. **I-3**, **I-4**, and **I-19**, although having a 3-methylthio group, gave relatively high reactivity, which showed that a suitable substituent on the aromatic ring also imposed a large effect.

Inhibitory Activities (in Vitro Activity) on Hill Reaction. The abilities of selected **I** compounds were evaluated as inhibitors of the photosynthetic electron transport by detecting their inhibiting effects on the Hill reaction. Photosynthetically active thylakoid membranes were used and isolated from spinach (*S. oleracea* L.) leaves. Observed IC_{50} data are listed in **Table 4**. Compounds **I-1** and **I-2** bearing a 4-chlorobenzyl group exhibited higher inhibitory activities than those bearing other aromatic compounds. Pyridine-containing compounds **I-3** to **I-9** and thiazole-containing compounds **I-10** to **I-20** showed a little lower activity than **I-1** and **I-2**, but much higher activity than other compounds. Substituents on aromatic ring showed obvious roles in activity. For example, compounds containing an alkoxy group at the pyridine or thiazole ring exhibited different inhibitory activities from halo-substituted analogues. R^2 did play an important role, but it was different from their in vivo data. From **Table 4**, the activities of most compounds bearing a methylthio group are a little higher than those of compounds bearing isopropyl.

Structure–Activity Relationships. To further explore the influence of aromatic rings and their substitutions on the activity, the analysis of the relationships between the structure and the in vitro activity was performed by CoMFA, which correlates the molecular interaction field differences with differences in the dependent target property. The cross-validation with LOO option and the SAMPLS program were used to determine the optimal number of components in CoMFA 3D-QSAR analyses, and then a non-cross-validated analysis was performed without column filtering. A model with q^2 (cross-validated r^2) = 0.565 and r^2 (non-cross-validated r^2) = 0.949, four components, was attained according to the definitions in SYBYL. The observed and calculated activity values are in **Table 4**. The models exhibited a good predictability on these compounds. 3D coefficient contour plots can view the field effect on the target property; they are helpful to identify important regions changing in the steric, electrostatic fields, and they may also help to identify the possible interaction sites. The compound **I-9** was illustrated to explain the field contributions of different properties obtained from the CoMFA analyses. The

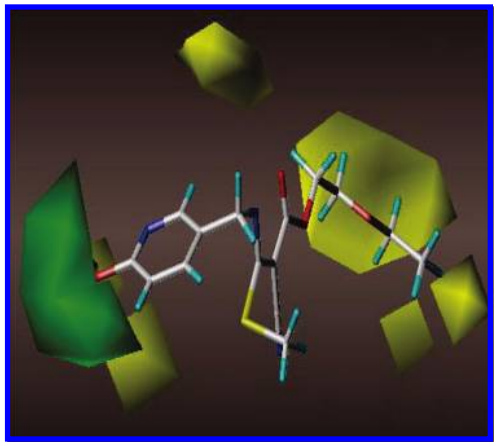

Figure 2. Steric maps from the CoMFA model. Compound **I-9** is shown inside the field. Sterically favored areas (contribution level of 80%) are represented by green polyhedra. Sterically disfavored areas (contribution level of 20%) are represented by yellow polyhedra.

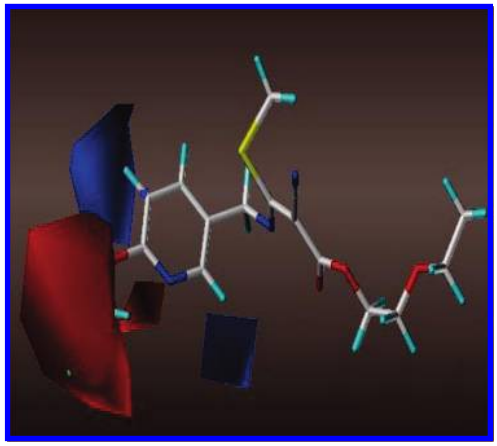

Figure 3. Electrostatic maps from the CoMFA model. Compound **I-9** is shown inside the field. Blue contours (80% contribution) encompass regions where an increase of positive charge will enhance affinity, whereas in red contoured areas (20% contribution) more negative charges are favorable.

steric and electrostatic contribution contour maps of CoMFA are plotted in **Figures 2** and **3**, respectively. The green and yellow polyhedra, in **Figure 2**, describe regions of space around the molecules where an increase in steric bulk enhances or diminishes the activity, respectively. Besides the yellow polyhedra surrounding the compound **I-9**, the most important characteritic of the figure is the green polyhedra on the para-position of the aromatic rings, which indicates that a bulky group on the para-substituent of aromatic rings is favorable, and the potency difference between compounds **I-12** and **I-20**, a change from a Br to a CF_3CH_2O group, can be explained. The electrostatic contour plots are shown in **Figure 3**. The red contour and the blue contour define regions of space where increasing electron density is favorable or disfavorable, respectively. A predominant feature of the electrostatic plot is the presence of a red contour surrounding the aromatic ring. It could be reasonably presumed that there is a significant electrostatic interaction between the aromatic ring and the possible receptor, and it may be assumed that the faction of receptor around the red region is electropositive or that there are hydrogen bonds between the inhibitors and the receptor. This is reflected in certain compounds, for example, **I-9** and **I-20**, which possess electronegative substituents on the aromatic ring and have high activity.

In summary, a series of novel 2-cyanoacrylates containing different aromatic rings were synthesized from arylmethylamine and alkyoxy- or methylthio-substituted cyanoacrylate with good yields, and their structures were characterized by ^{1}H NMR, elemental analysis, and single-crystal X-ray diffraction analysis. Their herbicidal activities against four weeds and inhibiting photosynthetic electron transport against isolated chloroplasts (the Hill reaction) were evaluated. In vivo data showed that most of the compounds showed greater herbicidal activities in postemergence treatment than in preemergence treatment. In postemergence treatment, most of the compounds exhibited higher herbicidal activities against dicotyledon weeds (rape and amaranth pigweed) than against monocotyledon weeds (alfalfa and hairy crabgrass). Both in vivo and in vitro data showed that the compounds containing benzene, pyridine, and thiazole moieties gave higher activities than those containing pyrimidine, pyridazine, furan, and tetrahedronfuran moieties. 3D-QSAR analysis based on in vitro data showed that a bulky and electronegative group around the para-position of the aromatic rings would have the potency to increase the activity, and further study is underway.

LITERATURE CITED

(1) Phillips, J. N.; Huppatz, J. L. Cyanoacrylate inhibitors of the Hill reaction III. Stereochemical and electronic aspects of inhibitor binding. *Z. Naturforsch.* **1984**, *39C*, 617–622.

(2) Huppatz, J. L.; Mcfadden, H. G.; Huber, M.-L.; McCaffery, L. F. Cyanoacrylate inhibitors of photosynthetic electron transport. Structural requirements for inhibitor potency and herbicidal activity. In *Synthesis and Chemistry of Agrochemicals III*; Baker, D. R., Fenyes, J. G., Steffens, J. J., Eds.; Maple Press: New York, 1992; pp 186−199.

(3) Mackay, S. P.; O'Malley, P. J. Molecular modelling of the interaction of cyanoacrylate inhibitors with photosystem II. Part I. *Z. Naturforsch.* **1993**, *48C*, 773–781.

(4) Huppatz, J. L. Quantifying the inhibitor−target site interactions of photosystem II herbicides. *Weed Sci.* **1996**, *44*, 743–748.

(5) Wang, Q.; Sun, H.; Cao, H.; Cheng, M.; Huang, R. Synthesis and herbicidal activity of 2-cyano-3-substituted-pyridinemethylaminoacrylates. *J. Agric. Food Chem.* **2003**, *51*, 5030–5035.

(6) Sun, H.; Wang, Q.; Huang, R.; Li, H.; Li, Y. Synthesis and biological activity of novel cyanoacrylates containing ferrocenyl moiety. *J. Organomet. Chem.* **2002**, *655*, 182.

(7) Wang, Q.; Li, H.; Cao, H.; Li, Y.; Huang, R. Synthesis and herbicidal activity of 2-cyano-3-(2-chlorothiazol-5-yl)methylaminoacrylates. *J. Agric. Food Chem.* **2004**, *52*, 1918–1922.

(8) Liu, Y.; Zhao, Q.; Wang, Q.; Li, H.; Huang, R.; Li, Y. Synthesis and herbicidal activity of 2-cyano-3-(2-fluoro-5-pyridyl)methylaminoacrylates. *J. Fluorine Chem.* **2005**, *126*, 345–348.

(9) Liu, Y.; Li, H.; Zhao, Q.; Wang, Q.; Huang, R. Synthesis and herbicidal activity of ethoxyethyl 2-cyano-3-(substituted)pyridinemethylamino-3-(substituted)acrylates. *Chin. J. Org. Chem.* **2006**, *26* (9), 1232–1238.

(10) Liu, Y.; Cai, B.; Li, Y.; Song, H.; Huang, R.; Wang, Q. Synthesis, crystal structure, and biological activities of 2-cyanoacrylates containing furan or tetrahydrofuran moieties. *J. Agric. Food Chem.* **2007**, *55*, 3011–3017.

(11) Yang, G. F.; Huang, X. Q. Development of quantitative structure-activity relationships and its application in rational drug design. *Curr. Pharm. Design* **2006**, *12* (35), 4601–4611.

(12) Windscheif, P. M.; Voegtle, F. Substituted dipyridylethenes and ethynes and key pyridine building blocks. *Synthesis* **1994**, *1*, 87–92.

(13) Kurkjy, R. P.; Brown, E. V. The preparation of thiazole grignard reagents and thiazolyllithium compounds. *J. Am. Chem. Soc.* **1952**, *74*, 6260–6262.

(14) Overend, W. G.; Wiggins, L. F. The conversion of sucrose into pyridazine derivatives. Part I. 3-Sulphanilamido-6-methylpyridazine. *J. Chem. Soc.* **1947**, *1*, 239–243.

(15) Schmidt-Nickels, W.; Johnson, T. B. Researches on pyrimidines. CXVIII. Molecular rearrangements in the thymine series. *J. Am. Chem. Soc.* **1930**, *52*, 4511–4516.

(16) Bedel, S.; Ulrich, G.; Picard, C. Alternative approach to the free radical bromination of oligopyridine benzylic-methyl group. *Tetrahedron Lett.* **2002**, *43* (9), 1697–1700.

(17) Holt, A. S.; French, C. S. Oxygen production by illuminated chloroplasts suspended in solution of oxidants. *Arch. Biochem.* **1948**, *19*, 368–378.

Received for review September 26, 2007. Revised manuscript received November 14, 2007. Accepted November 14, 2007. This work was supported by the National Key Project for Basic Research (2003CB114400), National Key Project of Scientific and Technical Supporting Programs (2006BAE01A01-5), and the National Natural Science Foundation of China (20421202) and Program for New Century Excellent Talents in University (NCET-04-0228).

JF072851X